
Gravity-driven Poiseuille Flow in Dilute Gases. Elastic and Inelastic Collisions

Andrés Santos¹ and Mohamed Tij²

¹ Departamento de Física, Universidad de Extremadura, E-06071 Badajoz, Spain
andres@unex.es

² Département de Physique, Université Moulay Ismaïl, Meknès, Morocco
mtij@fsmek.ac.ma

An overview of the hydrodynamic profiles derived by kinetic theory tools (Boltzmann equation and kinetic models) for the gravity-driven Poiseuille flow with particles colliding either elastically (planar and cylindrical geometries) or inelastically (planar geometry) is presented. The results obtained through second order in the gravity acceleration show that the Navier–Stokes predictions are qualitatively incorrect over distances of the order of the mean free path, especially in the case of the temperature profile.

1 Introduction

In the last decade, the Poiseuille flow generated by the action of a uniform longitudinal body force $m\mathbf{g}$ (e.g., gravity), rather than by a longitudinal pressure gradient, has received much attention from computational [1, 2, 3] and theoretical [3, 4, 5, 6, 7, 8, 9, 10, 11, 12] points of view. This interest has been fueled by the fact that the gravity-driven Poiseuille flow provides a nice example illustrating the limitations of the classical Navier–Stokes (NS) description, even in the bulk domain (i.e., far away from the boundary layers), over distances of the order of the mean free path. In contrast to what happens with the structure of a plane shock wave, where the NS discrepancies are essentially quantitative and are widely accounted for by the Burnett description [13], here the main failures of the NS predictions are qualitative and remain in the Burnett theory.

Kinetic theory analyses of the gravity-driven plane Poiseuille flow based on an expansion in powers of the gravity acceleration g [5, 6], on Grad’s moment method [3, 8], or on an expansion in powers of the Knudsen number [10], show that to second order in g the temperature profile includes a positive quadratic term in addition to the negative quartic term predicted by the NS (and Burnett) hydrodynamic equations. As a consequence of this extra term, the temperature does not present a flat maximum at the middle of the channel

but instead exhibits a *bimodal* shape with a local minimum surrounded by two symmetric maxima at a distance of a few mean free paths. The Fourier law is dramatically violated since in the slab enclosed by the two maxima the transverse component of the heat flux is parallel (rather than anti-parallel) to the thermal gradient. The kinetic theory prediction of a bimodal temperature profile in a slab has been confirmed by computer simulations [2, 3, 7]. A similar behavior occurs in the case of the Poiseuille flow in a pipe [9, 11].

For conventional gases under terrestrial conditions the interest of the Poiseuille flow induced by gravity is rather academic. However, this is not necessarily so when dealing with a “granular” gas [14], i.e., a collection of a large number of discrete solid particles (or grains) in a fluidized state such that each particle moves freely and independently of the rest, except for the occurrence of *inelastic* binary collisions. A kinetic theory study of a gas of inelastic hard spheres in a slab under the action of a longitudinal force and excited by a white noise “heating” has recently been undertaken [12].

The aim of this paper is to provide an overview of the hydrodynamic profiles derived by kinetic theory tools (Boltzmann equation and kinetic models) for the gravity-driven Poiseuille flow in the cases of particles colliding either elastically (planar and cylindrical geometries) or inelastically (planar geometry). The problem is presented in Sect. 2 and the NS solution to order g^2 is given in Sect. 3. The kinetic theory description for elastic and inelastic collisions is provided in Sects. 4 and 5, respectively. Finally, the main conclusions are briefly presented in Sect. 6.

2 Statement of the Problem

Let us consider a monodisperse dilute gas of identical spherical particles of mass m . The interaction among particles is assumed to reduce to binary collisions which can be either elastic or inelastic. In the first case, the (local) kinetic energy per unit volume is preserved by collisions. On the other hand, if the collisions are inelastic, energy is dissipated into the internal degrees of freedom; we will assume that this *internal* energy sink is counterbalanced by an *external* energy source produced by some sort of driving (e.g., boundary vibrations, external thermostats, ...). In addition, the system is under the influence of a constant gravitational field characterized by the acceleration vector \mathbf{g} . Under the above conditions, the macroscopic balance equations for the local densities of mass, momentum, and energy read

$$D_t n + n \nabla \cdot \mathbf{u} = 0, \quad D_t \mathbf{u} + \frac{1}{mn} \nabla \cdot \mathbf{P} = \mathbf{g}, \quad (1)$$

$$D_t T + \frac{2}{3n} (\nabla \cdot \mathbf{q} + \mathbf{P} : \nabla \mathbf{u}) = -(\zeta - \gamma) T. \quad (2)$$

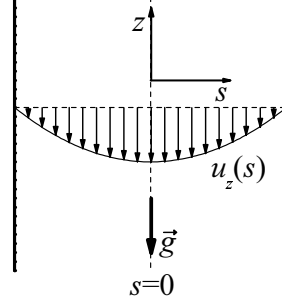


Fig. 1. Sketch of the longitudinal section of the Poiseuille flow induced by a gravitational force. In the planar geometry, the boundaries are infinite parallel plates and the variable s represents the Cartesian coordinate y . In the cylindrical geometry, the boundary is an infinite cylindrical surface and the variable s represents the radial coordinate r

In these equations, $D_t \equiv \partial_t + \mathbf{u} \cdot \nabla$ is the material time derivative, n is the number density, \mathbf{u} is the mean velocity, T is the temperature,³ \mathbf{P} is the pressure or stress tensor, and \mathbf{q} is the heat flux. The trace of the pressure tensor defines the hydrostatic pressure $p = \frac{1}{3}\text{Tr } \mathbf{P}$, which in a dilute gas is related to the density and the temperature through the ideal gas equation of state $p = nT$. In (2), $\zeta \geq 0$ is the (local) “cooling” rate associated with the collisional inelasticity and $\gamma \geq 0$ is the (local) “heating” rate associated with the external driving. If the collisions are elastic, the cooling rate vanishes ($\zeta = 0$) and no energy needs to be externally injected into the system ($\gamma = 0$). On the other hand, in the case of inelastic collisions one has $\zeta > 0$ and we will assume that the external source of energy compensates *locally* for the collisional cooling, i.e., $\gamma = \zeta$.

Now we particularize to the gravity-driven Poiseuille flow. In the planar geometry, the gas is enclosed between two infinite parallel plates normal to the y -axis and the acceleration of gravity $\mathbf{g} = -g\hat{\mathbf{z}}$ is applied along a direction $\hat{\mathbf{z}}$ parallel to the plates. A longitudinal section of the system is sketched in Fig. 1, where the variable s refers to the coordinate y . In the stationary laminar state the macroscopic variables depend on the variable y only, so the balance equations (1) and (2) yield

$$\frac{\partial P_{yy}}{\partial y} = 0, \quad \frac{\partial P_{yz}}{\partial y} = -\rho g, \quad P_{yz} \frac{\partial u_z}{\partial y} + \frac{\partial q_y}{\partial y} = 0, \quad (3)$$

where $\rho = mn$ is the mass density and use has been made of the assumptions $\zeta = \gamma = 0$ (elastic collisions) or $\zeta = \gamma > 0$ (inelastic collisions). Equations (3) imply that the normal stress P_{yy} is uniform across the system. Note that

³ We have set the Boltzmann constant equal to 1, so that T (which is usually termed “granular temperature” in the case of inelastic collisions) has dimensions of an energy.

neither the other two normal stresses P_{xx} and P_{zz} nor the longitudinal component q_z of the heat flux appear explicitly in the balance equations (3).

The Poiseuille flow can also be defined in a cylindrical geometry. In that case, the gas is inside an infinitely long straight tube of circular cross section, parallel to the z -axis. Figure 1 also represents a longitudinal section of the system, except that now the variable s refers to the radial coordinate $r = \sqrt{x^2 + y^2}$. Assuming again a stationary laminar flow, the only relevant spatial variable is r . Expressing the pressure tensor and the heat flux in cylindrical coordinates, the balance equations (1) and (2) reduce to [9, 11]

$$\frac{\partial}{\partial r}(rP_{rr}) = P_{\phi\phi}, \quad \frac{1}{r}\frac{\partial}{\partial r}(rP_{rz}) = -\rho g, \quad P_{rz}r\frac{\partial u_z}{\partial r} + \frac{\partial}{\partial r}(rq_r) = 0. \quad (4)$$

Our aim is to get the hydrodynamic profiles $p(s) = n(s)T(s)$, $u_z(s)$, and $T(s)$ (where $s = y$ and $s = r$ for the planar and cylindrical geometries, respectively) in the *bulk* domain, i.e., around $s = 0$, by a perturbation expansion through second order in g .

3 Navier–Stokes Theory

Equations (3) (planar case) and (4) (cylindrical case) do not constitute a closed set of equations. In a purely hydrodynamic approach, they must be complemented by constitutive relations expressing the fluxes \mathbf{P} and \mathbf{q} in terms of the hydrodynamic fields and their gradients.

If the gravity field were switched off ($g = 0$), the physical solution to (3) and (4) would correspond to an isotropic and uniform state, i.e., $\nabla p = \nabla T = \nabla \mathbf{u} = \mathbf{0}$, $\mathbf{P} = p\mathbf{I}$ (where \mathbf{I} is the unit tensor), and $\mathbf{q} = \mathbf{0}$. This is not but the equilibrium state in the case of elastic collisions and a uniformly heated non-equilibrium steady state in the case of inelastic collisions. On the other hand, the existence of the constant field g , no matter how small it is, induces gradients along the directions normal to the boundaries. It seems then quite natural that a Navier–Stokes (NS) description might be appropriate, at least for asymptotically small values of g . As will be seen, this expectation turns out not to hold true.

In a monodisperse gas, the NS equations follow from Newton’s viscosity law and Fourier’s heat conduction law,

$$\mathbf{P} = p\mathbf{I} - \eta \left[\nabla \mathbf{u} + (\nabla \mathbf{u})^\dagger - \frac{2}{3}(\nabla \cdot \mathbf{u})\mathbf{I} \right], \quad \mathbf{q} = -\kappa \nabla T - \mu \nabla n, \quad (5)$$

where the dagger denotes the transpose, η is the shear viscosity, κ is the thermal conductivity, and μ is a coefficient that vanishes if the collisions are elastic but is in general non-zero in granular gases. The expressions of the transport coefficients η and κ in terms of the temperature and the mechanical properties of the particles are well known in the case of elastic systems [15].

Moreover, η , κ , and μ have been derived for inelastic hard spheres [16, 17] and inelastic Maxwell particles [18] in the free cooling case as well as under heating.

Since in the Poiseuille flow the gradients are normal to the flow direction, it follows from (5) that the three normal stresses are identical. In Cartesian and cylindrical coordinates,

$$P_{xx} = P_{yy} = P_{zz} = p, \quad P_{\phi\phi} = P_{rr} = P_{zz} = p, \quad (6)$$

respectively. Equations (3) or (4) then imply that $p = \text{const}$, so that the (modified) Fourier law in (5) becomes

$$\mathbf{q} = -\kappa' \nabla T, \quad (7)$$

where we have called $\kappa' \equiv \kappa - n\mu/T$. Moreover, there does not exist a longitudinal component of the heat flux.

When the NS constitutive relations (5) are used in the balance equations (3) for the planar case, one gets the closed set of equations

$$\frac{\partial}{\partial y} \eta \frac{\partial u_z}{\partial y} = \frac{mpg}{T}, \quad \frac{\partial}{\partial y} \kappa' \frac{\partial T}{\partial y} = -\eta \left(\frac{\partial u_z}{\partial y} \right)^2. \quad (8)$$

Equations (8) give a parabolic-like velocity profile, that is characteristic of the Poiseuille flow, and a quartic-like shape for the temperature profile. Strictly speaking, these NS profiles are more complicated than just polynomials due to the temperature dependence of the transport coefficients. The knowledge of such a dependence is needed in order to get the NS hydrodynamic profiles from (8). However, if one is interested in those profiles to second order in g , the precise dependence of η and κ' on T is not needed and one can replace $\eta \rightarrow \eta_0$ and $\kappa' \rightarrow \kappa'_0$.⁴ More explicitly, the solution to (8) through order g^2 is

$$u_z(y) = u_0 + \frac{\rho_0 g}{2\eta_0} y^2 + O(g^3), \quad p(y) = p_0, \quad (9)$$

$$T(y) = T_0 \left(1 - \frac{\rho_0^2 g^2}{12\eta_0 \kappa'_0 T_0} y^4 \right) + O(g^4). \quad (10)$$

The shear stress and the heat flux are

$$P_{yz}(y) = -\rho_0 g y \left(1 + \frac{\rho_0^2 g^2}{60\eta_0 \kappa'_0 T_0} y^4 \right) + O(g^5), \quad (11)$$

$$q_y(y) = \frac{\rho_0^2 g^2}{3\eta_0} y^3 + O(g^4), \quad q_z(y) = 0, \quad (12)$$

⁴ Henceforth the subscript 0 attached to a quantity will denote the value of that quantity at the mid plane $y = 0$ or at the symmetry axis $r = 0$.

respectively. Note that the knowledge of the temperature profile to $O(g^2)$ allows us to get P_{xy} to $O(g^3)$ through (3). Equation (10) shows that the NS solution predicts that the temperature has a maximum at $y = 0$.

In the cylindrical case, insertion of (5) into (4) yields

$$r^{-1} \frac{\partial}{\partial r} \left(\eta r \frac{\partial u_z}{\partial r} \right) = \frac{m p g}{T}, \quad r^{-1} \frac{\partial}{\partial r} \left(\kappa' r \frac{\partial T}{\partial r} \right) = -\eta \left(\frac{\partial u_z}{\partial r} \right)^2. \quad (13)$$

Again, these two equations can be easily solved to second order in g :

$$u_z(r) = u_0 + \frac{\rho_0 g}{4\eta_0} r^2 + \mathcal{O}(g^3), \quad p(r) = p_0, \quad (14)$$

$$T(r) = T_0 \left(1 - \frac{1}{64} \frac{\rho_0^2 g^2}{\eta_0 \kappa'_0 T_0} r^4 \right) + \mathcal{O}(g^4). \quad (15)$$

The corresponding expressions for the shear stress and the heat flux are

$$P_{rz}(r) = -\frac{\rho_0 g}{2} r \left(1 + \frac{1}{192} \frac{\rho_0^2 g^2}{\eta_0 \kappa'_0 T_0} r^4 \right) + \mathcal{O}(g^5), \quad (16)$$

$$q_r(r) = \frac{\rho_0^2 g^2}{16\eta_0} r^3 + \mathcal{O}(g^4), \quad q_z(r) = 0, \quad (17)$$

respectively. Equation (15) implies that the temperature is maximum at $r = 0$.

4 Kinetic Theory Description. Elastic Collisions

In a kinetic theory approach the relevant information of the system is conveyed by the one-particle velocity distribution function $f(\mathbf{r}, \mathbf{v}, t)$. Its temporal evolution is governed by the non-linear Boltzmann equation [15], which in standard notation reads

$$\frac{\partial}{\partial t} f + \mathbf{v} \cdot \nabla f + \mathbf{g} \cdot \frac{\partial}{\partial \mathbf{v}} f = J[f, f], \quad (18)$$

where $J[f, f]$ is the collision operator for elastic collisions and we have assumed that no external forcing exists, apart from gravity. The influence of the interaction potential appears in $J[f, f]$ through the dependence of the collision rate on the relative velocity and the scattering angle. The hydrodynamic variables and their fluxes are just velocity moments of the distribution function:

$$\{n, n\mathbf{u}, p, \mathbf{P}, \mathbf{q}\} = \int d\mathbf{v} \left\{ 1, \mathbf{v}, \frac{m}{3} V^2, m\mathbf{V}\mathbf{V}, \frac{m}{2} V^2 \mathbf{V} \right\} f, \quad (19)$$

where the peculiar velocity $\mathbf{V} = \mathbf{v} - \mathbf{u}$ has been introduced as the velocity of a particle relative to the flow velocity. The exact balance equations (1) and (2), with $\zeta = \gamma = 0$, follow from (18) by taking velocity moments.

4.1 Planar Geometry

In the case of the stationary Poiseuille flow in a channel, the Boltzmann equation (18) becomes

$$\left(v_y \frac{\partial}{\partial y} - g \frac{\partial}{\partial v_z} \right) f = J[f, f] . \quad (20)$$

Strictly speaking, (20) must be supplemented by the appropriate boundary conditions describing the interaction of the particles with the plates. However, we are interested in the *bulk* region of the system, sufficiently far from the boundaries. Therefore, we will look for the Hilbert-class or *normal* solution to (20), namely a solution where all the spatial dependence of the distribution function takes place through a *functional* dependence of f on the hydrodynamic fields n , \mathbf{u} , and T .

Since the hydrodynamic variables of the gas and the associated fluxes are the first few moments of the distribution function f , it is convenient to consider the hierarchy of moment equations stemming from the Boltzmann equation (20). A moment of an arbitrary degree $k = k_1 + k_2 + k_3$ is defined as

$$M_{k_1, k_2, k_3}(y; g) = \int d\mathbf{v} V_x^{k_1} V_y^{k_2} V_z^{k_3} f(y, \mathbf{v}; g) . \quad (21)$$

Because of the symmetry properties of the problem, M_{k_1, k_2, k_3} is a function of y of the same parity as k_2 . Seen as a function of g , M_{k_1, k_2, k_3} has the same parity as k_3 . Finally, $M_{k_1, k_2, k_3} = 0$ if k_1 is odd. From (20) one gets the hierarchy

$$\frac{\partial}{\partial y} M_{k_1, k_2+1, k_3} + k_3 \left(\frac{\partial u_z}{\partial y} M_{k_1, k_2+1, k_3-1} + g M_{k_1, k_2, k_3-1} \right) = J_{k_1, k_2, k_3} , \quad (22)$$

where J_{k_1, k_2, k_3} is a collisional moment. In general, it involves all the velocity moments of the distribution, including those of a higher degree, and its explicit expression in terms of those moments is unknown. An important exception is provided by the Maxwell interaction potential, in which case the collision rate is independent of the velocity and, as a consequence, J_{k_1, k_2, k_3} can be expressed as a bilinear combination of moments of the same or smaller degree.

Even in the case of Maxwell molecules, the hierarchy (22) couples moments of a certain degree k to moments of degree $k+1$.⁵ However, the problem can be solved by a recursive scheme [6]. First, the moments are expanded in powers of g around a reference equilibrium state parameterized by u_0 , p_0 , and T_0 :

$$u_z(y; g) = u_0 + \sum_{\ell=1}^{\infty} u_z^{(\ell)}(y) g^\ell , \quad p(y; g) = p_0 + \sum_{\ell=2}^{\infty} p^{(\ell)}(y) g^\ell , \quad (23)$$

⁵ In what follows, we will use the roman boldface \mathbf{k} to denote the triad $\{k_1, k_2, k_3\}$ and the italic lightface k to denote the sum $k_1 + k_2 + k_3$.

$$T(y; g) = T_0 + \sum_{\ell=2}^{\infty} T^{(\ell)}(y) g^{\ell}, \quad M_{\mathbf{k}}(y; g) = M_{\mathbf{k}}^{(0)} + \sum_{\ell=1}^{\infty} M_{\mathbf{k}}^{(\ell)}(y) g^{\ell}. \quad (24)$$

Due to symmetry reasons, $u_z^{(\ell)}(y) = 0$ if $\ell = \text{even}$, $p^{(\ell)}(y) = T^{(\ell)}(y) = 0$ if $\ell = \text{odd}$, and $M_{\mathbf{k}}^{(\ell)}(y) = 0$ if $k_3 + \ell = \text{odd}$. The second step consists of the ansatz that the coefficients have just a polynomial dependence on y , namely

$$u_z^{(\ell)}(y) = \sum_{j=1}^{\ell} u_z^{(\ell, 2j)} y^{2j}, \quad p^{(\ell)}(y) = \sum_{j=2}^{\ell} p^{(\ell, 2j)} y^{2j}, \quad (25)$$

$$T^{(\ell)}(y) = \sum_{j=2}^{\ell} T^{(\ell, 2j)} y^{2j}, \quad M_{\mathbf{k}}^{(\ell)}(y) = \sum_{j=0}^{N_{\ell}} M_{\mathbf{k}}^{(\ell, j)} y^j, \quad (26)$$

where $N_1 = 1$ and $N_{\ell} = 2\ell$ for $\ell \geq 2$. Symmetry implies that $M_{\mathbf{k}}^{(\ell, j)} = 0$ if $k_2 + j = \text{odd}$. The numerical coefficients $u_z^{(\ell, 2j)}$, $p^{(\ell, 2j)}$, $T^{(\ell, 2j)}$, and $M_{\mathbf{k}}^{(\ell, j)}$ are determined recursively by inserting (23)–(26) into (22) and equating the coefficients of the same powers in g and y in both sides. This yields a hierarchy of *linear* equations for the unknowns. This rather cumbersome scheme has been solved through order g^2 in [6]. The results for the hydrodynamic profiles and the fluxes are

$$u_z(y) = u_0 + \frac{\rho_0 g}{2\eta_0} y^2 + O(g^3), \quad p(y) = p_0 \left[1 + C_p \left(\frac{mg}{T_0} \right)^2 y^2 \right] + O(g^4), \quad (27)$$

$$T(y) = T_0 \left[1 - \frac{\rho_0^2 g^2}{12\eta_0 \kappa_0 T_0} y^4 + C_T \left(\frac{mg}{T_0} \right)^2 y^2 \right] + O(g^4), \quad (28)$$

$$P_{zz}(y) = p_0 \left[1 + \frac{7}{3} C_p \left(\frac{mg}{T_0} \right)^2 y^2 + C_{\varpi} \frac{\rho_0 \eta_0^2 g^2}{p_0^3} \right] + O(g^4), \quad (29)$$

$$P_{yy} = p_0 \left(1 - C'_{\varpi} \frac{\rho_0 \eta_0^2 g^2}{p_0^3} \right) + O(g^4), \quad (30)$$

$$P_{yz}(y) = -\rho_0 g y \left[1 + \frac{\rho_0^2 g^2}{60\eta_0 \kappa_0 T_0} y^4 + \frac{C_p - C_T}{3} \left(\frac{mg}{T_0} \right)^2 y^2 \right] + O(g^5), \quad (31)$$

$$q_y(y) = \frac{\rho_0^2 g^2}{3\eta_0} y^3 + O(g^4), \quad q_z(y) = C_q m g \kappa_0 + O(g^3). \quad (32)$$

The numerical values of the coefficients C_p , C_T , C_{ϖ} , C'_{ϖ} , and C_q are displayed in Table 1. Comparison of (27)–(32) with the NS predictions (6) and (9)–(12) shows that the NS approach fails to account for the non-zero values of those five coefficients. At a qualitative level, the main contrast appears for the temperature profile. While, according to the NS equations, the temperature has a maximum at the mid plane $y = 0$, the Boltzmann equation shows that,

because of the extra quadratic term headed by C_T , the temperature actually presents a local minimum T_0 at $y = 0$ surrounded by two symmetric maxima T_{\max} at $y = \pm y_{\max}$, where $y_{\max} \equiv \sqrt{6C_T\eta_0\kappa_0 T_0}/p_0$. The relative height of the maxima is $(T_{\max} - T_0)/T_0 = 2C_T(gy_{\max}/v_0^2)^2$, where $v_0 = \sqrt{2T_0/m}$ is the thermal velocity at $y = 0$. If one defines an effective mean free path as $\lambda = 16\sqrt{2\eta\kappa T/15\pi}/5p$,⁶ one can write $y_{\max} = (15\sqrt{5\pi C_T}/16)\lambda_0 \simeq 3.74\lambda_0$, $(T_{\max} - T_0)/T_0 = (1125\pi C_T^2/128)(g\lambda_0/v_0^2)^2 \simeq 28.46(g\lambda_0/v_0^2)^2$.

Table 1. Numerical values of the coefficients C_p , C_T , C_ϖ , C'_ϖ , and C_q , both in the planar and the cylindrical geometries, according to the Navier–Stokes description (NS), the Boltzmann equation for Maxwell molecules (B-M), and the Bhatnagar–Gross–Krook kinetic model for any interaction (BGK)

coefficient	planar			cylindrical		
	NS	B-M	BGK	NS	B-M	BGK
C_p	0	1.2	1.2	0	0.3	0.3
C_T	0	1.0153	0.76	0	0.19429	0.14
C_ϖ	0	6.4777	13.12	0	3.4776	7.36
C'_ϖ	0	6.2602	12.24	0	1.7388	3.68
C_q	0	0.4	0.4	0	0.4	0.4

Equations (27)–(32) are exact in the context of the Boltzmann equation for Maxwell molecules. For more realistic potentials (e.g., hard spheres) the hierarchy (22) cannot be solved recursively, so that the problem must be addressed by means of approximations. One theoretical possibility is to consider the Chapman–Enskog expansion and retain as many terms as needed to get the profiles through order g^2 , but this is not very practical. The coefficients C_p and C_q are already captured by the Burnett description [6, 7], and so the Maxwell values $C_p = \frac{6}{5} = 1.2$ and $C_q = \frac{2}{5} = 0.4$ can be expected to be good approximations for other potentials. On the other hand, the determination of C_T , C_ϖ , and C'_ϖ requires the consideration of super-Burnett and super-super-Burnett contributions [6]. A second approach is Grad’s moment method [19]. The thirteen-moment approximation [3] yields (27)–(32) with $C_p = \frac{6}{5}$, $C_q = \frac{2}{5}$, $C_T = \frac{14}{25} = 0.56$, and $C_\varpi = C'_\varpi = 0$, irrespective of the interaction potential. On the other hand, the nineteen-moment approximation [8] gives $C_p = \frac{50998}{42025} \simeq 1.214$ and $C_T = \frac{208518}{210125} \simeq 0.992$ for hard spheres, while it predicts $C_p = \frac{6}{5}$ and $C_T = \frac{26}{25} = 1.04$ for Maxwell molecules. Comparison with the exact results $C_p = \frac{6}{5}$ and $C_T = 1.0153$ for Maxwell molecules suggests that the nineteen-moment approximation is rather accurate, although it overestimates C_T by a few percent.

An alternative route to get reasonable estimates with relatively much less effort than in the case of the Boltzmann equation consists of using a ki-

⁶ This definition guarantees that $\lambda = (\sqrt{2}\pi n\sigma^2)^{-1}$ for hard spheres of diameter σ .

netic model equation. The prototype kinetic model is the one proposed by Bhatnagar, Gross, and Krook (BGK) and, independently, by Welander and Kogan [20]. In this model, the Boltzmann collision operator is replaced by a relaxation-time term towards the local equilibrium state:

$$J[f, f] \rightarrow -\nu(f - f_\ell) , \quad f_\ell = n \left(\frac{m}{2\pi T} \right)^{3/2} \exp(-mV^2/2T) . \quad (33)$$

The BGK model has proven to be quite reliable in non-Newtonian shear flow problems [21]. The solution to the BGK equation for the plane Poiseuille flow has been explicitly obtained through order g^5 [5]. The results strongly suggest that the series expansion is only asymptotic, so that from a practical point of view one can focus on the first few terms. The results agree with the profiles (27)–(32), except that the numerical values of the coefficients C_T , C_ϖ , and C'_ϖ differ from those derived from the Boltzmann equation for Maxwell molecules, as shown in Table 1. The coefficient C_T in the BGK model is about 25% smaller than in the Boltzmann equation, while C_ϖ and C'_ϖ are about twice larger in the former than in the latter. Interestingly enough, the BGK value $C_T = \frac{19}{25} = 0.76$ agrees quite well with Monte Carlo simulations of the Boltzmann equation for hard spheres [2], even though the nineteen-moment method predicts $C_T \lesssim 0.99$.

4.2 Cylindrical Geometry

In the cylindrical Poiseuille flow, the Boltzmann equation (18) becomes

$$\left[v_r \frac{\partial}{\partial r} + \frac{v_\phi}{r} \left(v_\phi \frac{\partial}{\partial v_r} - v_r \frac{\partial}{\partial v_\phi} \right) - g \frac{\partial}{\partial v_z} \right] f = J[f, f] . \quad (34)$$

The algebra is now more involved than in the planar case, but still the hierarchy of moment equations can be recursively solved for Maxwell molecules through an expansion in powers of g . To second order, the solution is [11]

$$u_z(r) = u_0 + \frac{\rho_0 g}{4\eta_0} r^2 + O(g^3) , \quad p(r) = p_0 \left[1 + C_p \left(\frac{mg}{T_0} \right)^2 r^2 \right] + O(g^4) , \quad (35)$$

$$T(z) = T_0 \left[1 - \frac{\rho_0^2 g^2}{64\eta_0 \kappa_0 T_0} r^4 + C_T \left(\frac{mg}{T_0} \right)^2 r^2 \right] + O(g^4) , \quad (36)$$

$$P_{zz}(y) = p_0 \left[1 + \frac{7}{3} C_p \left(\frac{mg}{T_0} \right)^2 r^2 + C_\varpi \frac{\rho_0 \eta_0^2 g^2}{p_0^3} \right] + O(g^4) , \quad (37)$$

$$P_{rr}(r) = p_0 \left(1 + \frac{1}{6} C_p \left(\frac{mg}{T_0} \right)^2 r^2 - C'_\varpi \frac{\rho_0 \eta_0^2 g^2}{p_0^3} \right) + O(g^4) , \quad (38)$$

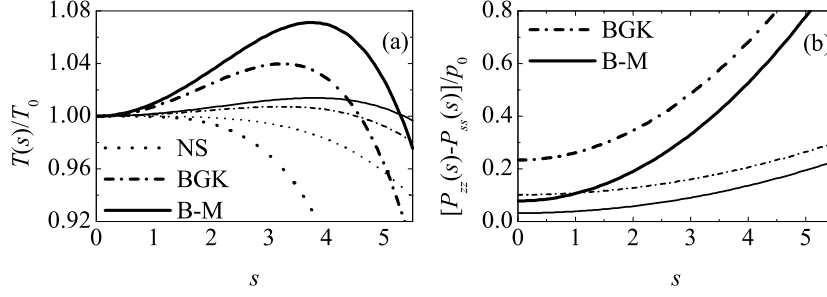


Fig. 2. Plot of (a) $T(s)/T_0$ and (b) $[P_{zz}(s) - P_{ss}(s)]/p_0$ for $g\lambda_0/v_0^2 = 0.05$ in the planar ($s = y$, *thick lines*) and cylindrical ($s = r$, *thin lines*) geometries, according to the NS equations (\cdots), the BGK model ($-\cdots-$), and the Boltzmann equation for Maxwell molecules ($—$)

$$P_{rz}(r) = -\frac{\rho_0 g}{2} r \left[1 + \frac{\rho_0^2 g^2}{192 \eta_0 \kappa_0 T_0} r^4 + \frac{C_p - C_T}{2} \left(\frac{mg}{T_0} \right)^2 r^2 \right] + O(g^5), \quad (39)$$

$$q_r(r) = \frac{\rho_0^2 g^2}{16 \eta_0} r^3 + O(g^4), \quad q_z(r) = C_q mg \kappa_0 + O(g^3). \quad (40)$$

The numerical values of the coefficients C_p , C_T , C_ϖ , C'_ϖ , and C_q for this case are again displayed in Table 1. As happened in the planar case, the temperature exhibits a non-monotonic profile: it has a local minimum T_0 at $r = 0$ and its maximum value T_{\max} is reached at $r = r_{\max}$, where $r_{\max} \equiv \sqrt{32 C_T \eta_0 \kappa_0 T_0 / p_0} = (5\sqrt{15\pi C_T / 4}) \lambda_0 \simeq 3.78 \lambda_0$. The relative value of the maximum is $(T_{\max} - T_0)/T_0 = 2C_T (gr_{\max}/v_0^2)^2 = (375\pi C_T^2 / 8) (g\lambda_0/v_0^2)^2 \simeq 5.56 (g\lambda_0/v_0^2)^2$. It is noteworthy that, expressed in the same units, r_{\max} is practically equal to y_{\max} , while $T_{\max} - T_0$ is about five times smaller in the cylindrical geometry than in the planar geometry.

The BGK model has been solved for the cylindrical Poiseuille flow through order g^4 [9], suggesting again an asymptotic character of the expansion. The resulting profiles agree with (35)–(40), but with different values of C_T , C_ϖ , and C'_ϖ (see Table 1). It is interesting to note that the ratios between the BGK and the B-M values for C_T , C_ϖ , and C'_ϖ are almost the same in the planar and the cylindrical geometries.

Figure 2 shows the profiles for the temperature and for the normal stress difference $P_{zz} - P_{ss}$ (where $P_{ss} = P_{yy}$ and $P_{ss} = P_{rr}$ in the planar and cylindrical geometries, respectively) for $g\lambda_0/v_0^2 = 0.05$.

5 Kinetic Theory Description. Inelastic Collisions

Now we consider the plane Poiseuille flow and assume that the particles are smooth *inelastic* hard spheres of diameter σ and coefficient of restitution $\alpha < 1$. In the dilute regime, the cooling rate is approximately given by [16, 22]

$$\zeta(\alpha) = \nu \frac{5}{12}(1 - \alpha^2) , \quad \nu \equiv \frac{16}{5} n \sigma^2 (\pi T/m)^{1/2} . \quad (41)$$

It is obvious that all the mathematical difficulties embodied in the Boltzmann equation for (elastic) hard spheres are further increased in the inelastic case. Therefore, in order to get explicit results with a reasonable amount of effort, it seems convenient to extend the BGK model (33) to the realm of inelastic collisions. The simplest possibility is perhaps [22, 23]

$$J[f, f] \rightarrow -\beta(\alpha)\nu(f - f_\ell) + \frac{\zeta(\alpha)}{2} \frac{\partial}{\partial \mathbf{v}} \cdot (\mathbf{V}f) , \quad (42)$$

where $\beta(\alpha)$ is a dimensionless function of the coefficient of restitution that can be freely chosen to optimize the agreement with the Boltzmann description. A simple choice is $\beta(\alpha) = \frac{1}{2}(1 + \alpha)$ [23]. Here, however, we will take $\beta(\alpha) = \frac{1}{6}(1 + \alpha)(2 + \alpha)$, which makes the BGK shear viscosity agree well with the Boltzmann one [22, 23]. Good quantitative agreement between the kinetic model (42) and the Boltzmann equation has been found for the simple shear and Couette flows [24].

As said in Sect. 2, an external energy input is needed to compensate for the collisional dissipation in order to reach a nonequilibrium steady state. In real experiments this is usually achieved by means of boundary vibrations of small amplitude and high frequency. However, this type of realistic heating through the boundaries is difficult to deal with at a theoretical level due to unavoidable boundary effects. These difficulties are overcome by assuming a *bulk* heating mechanism acting on all the particles simultaneously. The most commonly used type of bulk driving for inelastic particles consists of a stochastic force in the form of Gaussian white noise, which appears in the Boltzmann equation under the form of a diffusion term in velocity space [25]. In summary, our kinetic equation to describe the stationary plane Poiseuille flow reads [12]

$$\left(v_y \frac{\partial}{\partial y} - g \frac{\partial}{\partial v_z} - \frac{\gamma T}{2m} \frac{\partial^2}{\partial \mathbf{v}^2} \right) f = -\beta\nu(f - f_\ell) + \frac{\zeta}{2} \frac{\partial}{\partial \mathbf{v}} \cdot (\mathbf{V}f) , \quad (43)$$

where the heating rate γ is taken equal to ζ , as discussed in Sect. 2.

The perturbative solution of (43) is seen to agree with the structure of (27)–(32), except that now the NS transport coefficients η and $\kappa' = \kappa - n\mu/T$, as well as C_T , C_ϖ , and C_ϖ , are functions of the coefficient of restitution. As said above, the choice $\beta = \frac{1}{6}(1 + \alpha)(2 + \alpha)$ guarantees that the BGK shear viscosity η agrees with the one derived from the Boltzmann equation for inelastic hard spheres in the simplest Sonine approximation. However, as already happens in the elastic case, the (modified) thermal conductivity κ' differs in both kinetic equations. In order to circumvent this problem, once the BGK solution is expressed in terms of η and κ' , we will take for those coefficients the expressions obtained from the Boltzmann equation. In the case of a granular gas heated by the white noise forcing, the transport coefficients are approximately given by [17]

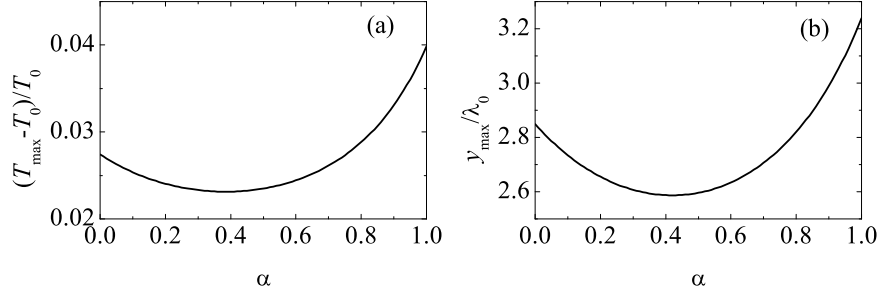


Fig. 3. Plot of (a) $(T_{\max} - T_0)/T_0$ for $g\lambda_0/v_0^2 = 0.05$ and (b) y_{\max}/λ_0 as functions of the coefficient of restitution α

$$\eta = \frac{p}{\nu} \frac{4}{(1+\alpha)(3-\alpha)}, \quad \kappa' = \frac{15p}{4m\nu} \frac{32}{(1+\alpha)(49-33\alpha)}. \quad (44)$$

While η monotonically increases with inelasticity, κ' starts decreasing with increasing inelasticity, reaches a minimum value around $\alpha \simeq 0.4$, and then slightly increases for $\alpha \gtrsim 0.4$. The expressions for $C_T(\alpha)$, $C_\varpi(\alpha)$, and $C'_\varpi(\alpha)$ are

$$C_T(\alpha) = \frac{1}{25} \frac{38 + 43\zeta^* + 17\zeta^{*2}}{(1+\zeta^*)(2+\zeta^*)}, \quad \zeta^* \equiv \frac{\frac{5}{12}(1-\alpha^2)}{\beta(\alpha) + \frac{5}{12}(1-\alpha^2)}, \quad (45)$$

$$C_\varpi(\alpha) = \frac{16}{25} \frac{82 + 67\zeta^* + 8\zeta^{*2}}{(1+\zeta^*)(2+\zeta^*)^2}, \quad C'_\varpi(\alpha) = \frac{12}{25} \frac{102 + 87\zeta^* + 13\zeta^{*2}}{(1+\zeta^*)(2+\zeta^*)^2}. \quad (46)$$

Of course, in the elastic limit ($\alpha \rightarrow 1$) the above coefficients reduce to the BGK values listed in Table 1. The coefficient $C_T(\alpha)$ monotonically decreases with increasing inelasticity. However, the non-monotonic behavior of $\kappa'(\alpha)$ makes the relative location of the maximum y_{\max}/λ_0 , where $\lambda_0 = (\sqrt{2}\pi n_0 \sigma^2)^{-1}$, as well as the relative height $(T_{\max} - T_0)/T_0$ for a given value of $g\lambda_0/v_0^2$, exhibit a non-monotonic behavior. This is illustrated in Fig. 3.

6 Conclusions

In this paper we have reviewed the main results derived within a kinetic theory framework for the steady Poiseuille flow driven by a uniform longitudinal force. The results are restricted to the bulk domain and are obtained by a perturbation expansion through second order. We have considered both elastic and inelastic particles. In the first case, the planar and the cylindrical geometries have been considered and the results are presented from the Boltzmann equation for Maxwell molecules as well as from the BGK kinetic model for any interaction. In the case of granular gases (inelastic collisions), however, only the planar geometry and a BGK-like kinetic model have been addressed.

In all the cases, the profiles of the hydrodynamic fields and their fluxes exhibit important deviations from the NS predictions: the hydrostatic pressure is not uniform, normal stress differences are present, a component of the heat flux normal to the thermal gradient exists, and the temperature profile has a non-monotonic shape. In general, those deviations are more important in the planar geometry than in the cylindrical one. For instance, the relative height of the maximum temperature, $(T_{\max} - T_0)/T_0$, is about five times larger in the former case than in the latter, even though the location of that maximum is similar in both cases, i.e., $y_{\max} \simeq r_{\max}$. It is worthwhile noting that the BGK model succeeds in capturing the functional form of the profiles derived from a more fundamental Boltzmann description, albeit with some changes in the numerical factors. Thus, the BGK model underestimates the maximum value T_{\max} , as well as its location y_{\max} or r_{\max} . Concerning the case of inelastic collisions, the results show a weak influence of the coefficient of restitution α . In any case, for small and moderate inelasticities (say $\alpha \gtrsim 0.5$) there is a slight decrease in the quantitative deviations from the NS profiles as inelasticity grows, while the opposite behavior takes place for high inelasticity ($\alpha \lesssim 0.5$).

References

1. Travis, K.P., Todd, B.D., Evans, D.J.: Poiseuille flow of molecular fluids. *Physica A*, **240**, 315–327 (1997); Todd, B.D., Evans, D.J.: Temperature profile for Poiseuille flow. *Phys. Rev. E*, **55**, 2800–2807 (1997).
2. Malek Mansour, M., Baras, F., Garcia, A.L.: On the validity of hydrodynamics in plane Poiseuille flows. *Physica A*, **240**, 255–267 (1997).
3. Risso D., Cordero, P.: Generalized hydrodynamics for a Poiseuille flow: theory and simulations. *Phys. Rev. E*, **58**, 546–553 (1998).
4. Alaoui, M., Santos, A.: Poiseuille flow driven by an external force. *Phys. Fluids A*, **4**, 1273–1282 (1992); Esposito, R., Lebowitz, J. L., Marra, R.: A hydrodynamic limit of the stationary Boltzmann equation in a slab. *Commun. Math. Phys.*, **160**, 49–80 (1994).
5. Tij, M., Santos, A.: Perturbation analysis of a stationary nonequilibrium flow generated by an external force. *J. Stat. Phys.*, **76**, 1399–1414 (1994).
6. Tij, M., Sabbane, M., Santos, A.: Nonlinear Poiseuille flow in a gas. *Phys. Fluids*, **10**, 1021–1027 (1998).
7. Uribe, F. J., Garcia, A. L.: Burnett description for plane Poiseuille flow. *Phys. Rev. E*, **60**, 4063–4078 (1999).
8. Hess, S., Malek Mansour, M.: Temperature profile of a dilute gas undergoing a plane Poiseuille flow. *Physica A*, **272**, 481–496 (1999).
9. Tij, M., Santos, A.: Non-Newtonian Poiseuille flow of a gas in a pipe. *Physica A*, **289**, 336–358 (2001).
10. Aoki, K., Takata, S., Nakanishi, T.: A Poiseuille-type flow of a rarefied gas between two parallel plates driven by a uniform external force. *Phys. Rev. E*, **65**, 026315 (2002).
11. Sabbane, M., Tij, M., Santos, A.: Maxwellian gas undergoing a stationary Poiseuille flow in a pipe. *Physica A*, **327**, 264–290 (2003).

12. Tij, M., Santos, A.: Poiseuille flow in a heated granular gas. *J. Stat. Phys.*, **117**, 901–928 (2004).
13. Montanero, J.M., López de Haro, M., Garzó, V., Santos, A.: Strong shock waves in a dense gas: Burnett theory versus Monte Carlo simulation. *Phys. Rev. E*, **58**, 7319–7324 (1998); Simple and accurate theory for strong shock waves in a dense hard-sphere fluid. *Ibid.*, **60**, 7592–7595 (1999).
14. Campbell, C.S.: Rapid granular flows. *Annu. Rev. Fluid Mech.*, **22**, 57–92 (1990); Jaeger, H.M., Nagel, S.R.: Granular solids, liquids, and gases. *Rev. Mod. Phys.*, **68**, 1259–1273 (1996); Kadanoff, L.P.: Built upon sand: Theoretical ideas inspired by granular flows. *Ibid.*, **71**, 435–444 (1996); Dufty, J.W.: Kinetic theory and hydrodynamics for a low density granular gas. *Adv. Compl. Syst.*, **4**, 397–406 (2001); Goldhirsch, I.: Rapid granular flows. *Annu. Rev. Fluid Mech.*, **35**, 267–293 (2003); Brilliantov, N., Pöschel, T.: *Kinetic Theory of Granular Gases*. Oxford University Press, Oxford (2004).
15. Chapman, S., Cowling, T.G.: *The Mathematical Theory of Nonuniform Gases*. Cambridge University Press, Cambridge (1970).
16. Brey, J.J., Dufty, J.W., Kim, C.S., Santos, A.: Hydrodynamics for granular flow at low density. *Phys. Rev. E*, **58**, 4638–4653 (1998).
17. Garzó, V., Montanero, J.M.: Transport coefficients of a heated granular gas. *Physica A*, **313**, 336–356 (2002).
18. Santos, A.: Transport coefficients of d -dimensional inelastic Maxwell models. *Physica A*, **321**, 442–466 (2003).
19. Grad, H.: On the kinetic theory of rarefied gases. *Commun. Pure Appl. Math.*, **2**, 331–407 (1949); Asymptotic theory of the Boltzmann equation. *Phys. Fluids*, **6**, 147–181 (1963).
20. Bhatnagar, P.L., Gross, E.P., Krook, M.: A model for collision processes in gases. I. Small amplitude processes in charged and neutral one-component systems. *Phys. Rev.*, **94**, 511–525 (1954); Welander, P.: On the temperature jump in a rarefied gas. *Arkiv Fysik*, **7**, 507–553 (1954); Kogan, N.: On the equations of motion of a rarefied gas. *Appl. Math. Mech.*, **22**, 597–607 (1958).
21. Garzó, V., Santos, A.: *Kinetic Theory of Gases in Shear Flows*. Nonlinear Transport. Kluwer, Dordrecht (2003).
22. Brey, J.J., Dufty, J.W., Santos, A.: Kinetic models for granular flow. *J. Stat. Phys.*, **97**, 281–322 (1999).
23. Santos, A., Astillero, A.: Can a system of elastic hard spheres mimic the transport properties of a granular gas?. *ArXiv: cond-mat/0405252*.
24. Brey, J.J., Ruiz-Montero, M.J., and Moreno, F.: Steady uniform shear flow in a low density granular gas. *Phys. Rev. E*, **55**, 2846–2856 (1997); Montanero, J.M., Garzó, V., Santos, A., Brey, J.J.: Kinetic theory of simple granular shear flows of smooth hard spheres. *J. Fluid Mech.*, **389**, 391–411 (1999); Tij, M., Tahiri, E.E., Montanero, J.M., Garzó, V., Santos, A., Dufty, J.W.: Nonlinear Couette flow in a low density granular gas. *J. Stat. Phys.*, **103**, 1035–1068 (2001).
25. van Noije, T.P.C., Ernst, M.H.: Velocity distributions in homogeneous granular fluids: the free and the heated case. *Gran. Matt.*, **1**, 57–64 (1998); Montanero, J.M., Santos, A.: Computer simulation of uniformly heated granular fluids. *Ibid.*, **2**, 53–64 (2000).